

B. TECH. PROJECT REPORT

On

Effect of Stator Design Parameters on PMSM Vibration

BY
Allam Dhanush 180003007
Saketh Reddy 180003060



DISCIPLINE OF MECHANICAL ENGINEERING
INDIAN INSTITUTE OF TECHNOLOGY INDORE
May 2022

Effect of Stator Design Parameters on PMSM Vibration

A PROJECT REPORT

*Submitted in partial fulfillment of the
requirements for the award of the degrees*

of
BACHELOR OF TECHNOLOGY
in

MECHANICAL ENGINEERING

Submitted by:

Allam Dhanush 180003007
Saketh Reddy 180003060

Guided by:

Dr. Anand Parey



INDIAN INSTITUTE OF TECHNOLOGY INDORE

May 2022

CANDIDATE'S DECLARATION

We hereby declare that the project entitled “**Effect of stator design parameters on PMSM vibration**” submitted in partial fulfillment for the award of the degree of Bachelor of Technology in Mechanical engineering completed under the supervision of **Dr. Anand Parey, Professor Mechanical Engineering, IIT Indore** is an authentic work.

Further, we declare that we have not submitted this work for the award of any other degree elsewhere.

Allam Dhanush
25-May-2022

Allam Dhanush

Saketh Reddy
25-05-2022

Saketh Reddy

CERTIFICATE by BTP Guide(s)

It is certified that the above statement made by the students is correct to the best of my knowledge.

Anand Parey

25-May-2022
Dr. Anand Parey
Professor

Preface

This report on “Effect of stator design parameters on PMSM vibration” is prepared under the guidance of Prof. Anand Parey.

Through this report we have tried to investigate the effect of parameters slot height and slot opening width on PMSM vibrations and motor performance.

Ansys electronics suit 19.2 is used to create the structural model and calculate electromagnetic forces. Ansys workbench 19.2 is used for modal analysis and harmonic response analysis.

We have tried to the best of our abilities and knowledge to explain the content in a lucid manner. We have also added 3-D models and figures to make it more illustrative.

Allam Dhanush & Saketh Reddy

B.Tech. IV Year

Discipline of Mechanical Engineering

IIT Indore

Acknowledgements

We wish to thank Prof. Anand Parey for his kind support and valuable guidance. It is his help and support, due to which we became able to complete the design and technical report.

We would also like to thank our friends and family for believing in us and providing us for whatever needed.

Allam Dhanush & Saketh Reddy
B.Tech. IV Year
Discipline of Mechanical Engineering
IIT Indore

Abstract

Environmental pollution, fossil fuel depletion, and global warming are some of the problems with conventional internal combustion engines that have sparked interest in electric vehicles. Traction source for electric vehicles is the electric motor. An electric vehicle can employ a variety of electric motors. Permanent magnet synchronous motors (PMSM) are commonly utilized in electric vehicles because of their high-power density, high efficiency, and low vibration and noise with high performance. Electric motor is one of the major contributors to vibration and noise in electric vehicles. Apart from the low-frequency noise produced by the conventional internal combustion engines, the electric motor produces high-frequency noise. Because the human ear is extremely sensitive in this frequency range, a severe noise sensation may result. Hence it is crucial to control vibration and noise in electric motor. Since noise is produced by vibrating surfaces, the vibration characteristics of the PMSM deserves attention. The goal of our project is to study different vibration mechanisms and solutions available in the literature for vibration control. Investigating the effect of stator design parameters on PMSM vibration is the main objective of our work.

The parameters slot height and slot opening width are chosen for investigation in this work. To investigate the influence of slot height and slot opening width, three stator models with varying values of slot height and three stator models with varying values of slot opening width were built. Vibration analysis was performed on all models. The vibration analysis results of each model were compared to determine the effect of a design parameter on vibration.

Keywords: Vibration and Noise, PMSM, Slot height, Slot opening width, Vibration analysis.

Table of contents

Candidate’s Declaration.....	I
Supervisor’s Certificate.....	I
Preface.....	II
Acknowledgements.....	III
Abstract.....	IV
1. Introduction.....	1
2. Literature Review.....	3
3. Objectives.	5
4. Vibration and Noise in PMSM.	6
4.1 Sources of vibrations and noise in PMSM.....	6
4.2 Electromagnetic vibration classification.....	6
4.3 Vibration analysis methods.....	7
4.4 Electromagnetic vibration and noise reduction.....	8
5. Simulation.	10
5.1 Methodology.....	10
5.2 Simulation details.....	11
6. Results and Discussions.	13
6.1 Modal analysis.....	13
6.2 Amplitude of vibration and motor performance.....	14
6.3 Deformation images.....	16
6.4 Radial electromagnetic force.....	18
6.5 Airgap magnetic flux density.....	19
7. Conclusions and Scope for Future Work.	21
7.1 Conclusions	21
7.2 Scope for future work.....	21
References.....	22

List of Figures

1. Figure 1a: schematic of radial flux PMSM.
2. Figure 1b: schematic of axial flux PMSM.
3. Figure 1c: radial flux PMSM 3D modal.
4. Figure 2a: PMSM stator.
5. Figure 2b: stator slot geometry.
6. Figure 3: flow chart of vibration analysis.
7. Figure 4: Ansys workbench analysis setup.
8. Figure 5: PMSM stator modal in 3D.
9. Figure 6: amplitude of vibration variation with slot height.
10. Figure 7: amplitude of vibration variation with slot opening width.
11. Figure 8a: maximum deformation images for slot height 16.5mm.
12. Figure 8b: maximum deformation images for slot height 17mm.
13. Figure 8c: maximum deformation images for slot height 17.5mm.
14. Figure 9a: maximum deformation images for slot opening width 10mm.
15. Figure 9b: maximum deformation images for slot opening width 11mm.
16. Figure 9c: maximum deformation images for slot opening width 12mm.
17. Figure 10: radial force variation with slot height.
18. Figure 11: radial force variation with slot opening width.
19. Figure 12: magnitude of airgap magnetic flux density variation with slot height.
20. Figure 13: mag_B variation in angle range of 45.18 deg to 60.02 deg.
21. Figure 14: magnitude of airgap magnetic flux density variation with slot height.

List of Tables

1. Table 1: comparison of electric motors.
2. Table 2a: design parameter values for slot height variation.
3. Table 2b: design parameter values for slot opening width variation.
4. Table 3: modal analysis results for slot height variation.
5. Table 4: modal analysis results for slot opening width variation.
6. Table 5: motor performance variation with slot height.
7. Table 6: motor performance variation with slot opening width

1. INTRODUCTION

Environmental pollution, fossil fuel depletion, and global warming are some of the problems associated with the operation of conventional internal combustion engines (ICE) that have sparked interest in electric vehicles (EVs) and hybrid electric vehicles (HEVs).

Traction source in EVs and HEVs is electric motor. Depending on the cost, controllability, efficiency, power density and installation space different types of electric motors are used in electric vehicles. Direct current motors (DC), induction motors (IM), permanent magnet synchronous motors (PMSM), and switching reluctance motors (SRM). are the four main types of electric motors used in electric vehicles.

DC motors are inexpensive, have simple controllability and do not require complex power electronics, but they have a poor overload capacity due to high rotor losses and grow in size for high power applications. IMs are most suitable for a series hybrid system. Induction motors have a wide speed range and good efficiency at high speed. The disadvantages of IMs are a low overload capacity due to rotor losses. PMSMs are suitable for parallel hybrid system. PMSMs have high efficiency in the nominal speed range, because of its high-power density PMSMs are best suited for systems with limited installation area. Because of high cost of magnets used in PMSMs they are more expensive when compared to other motors. SRMs are inexpensive, require low maintenance and have a simple construction. SRM generate high noise and torque ripple, and their control is complicated because of high non linearity.

Table 1: comparison of electric motors.
(‘+’ denotes advantage, ‘-’ denotes disadvantage, ‘0’ denotes neutral)

CRITERIA	Types of motor			
	DC	IM	PMSM	SRM
Power density	-	0	++	0
Efficiency	-	+	++	-
Vibration and noise	-	++	++	--
Simplicity	++	+	0	++
Controllability	++	+	+	-
Cost	+	+	-	+
Space	-	+	++	+

PMSM is one of the most suited motors for electric vehicles due to its high-power density, high efficiency, and low vibration and noise production at high performance. Because PMSM is widely employed in electric vehicles, it is chosen for investigation in this project.

Depending on the magnetic flux direction PMSM are divided into two types: radial flux and axial flux motors as shown in fig 1(a) and 1(b). Radial flux PMSM is taken into account in this project.

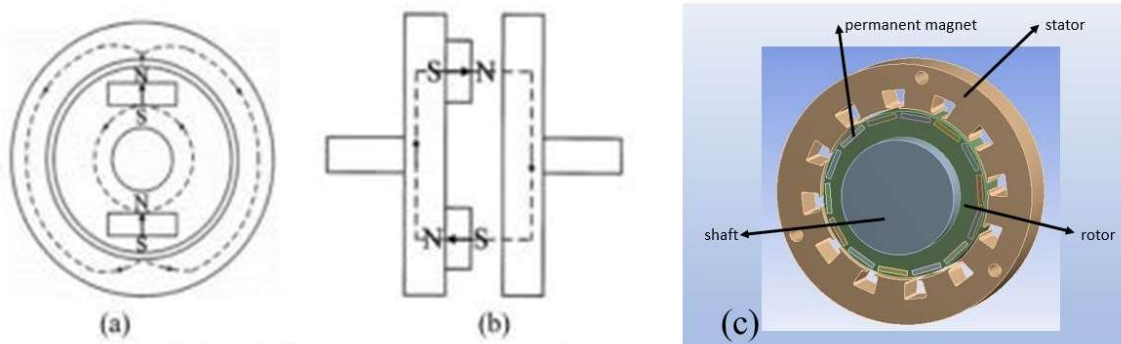


Fig1: (a)schematic of radial flux PMSM. (b)schematic of axial flux PMSM.
(c)radial flux PMSM 3D model.

Engineers and designers are interested in vibration and noise because they can have a substantial impact on a vehicle's driving comfort. As environmental awareness has grown noise has been recognized as a form of pollution. As a result, low-noise vehicles are becoming increasingly popular. Because of these requirements, vibration and noise reduction has emerged as a critical research topic.

Electric motor is the major noise source in electric vehicles. Apart from the low-frequency noise produced by the conventional internal combustion engines, the electric motor produces high-frequency noise ranging from 400 to 2000 Hz. Because the human ear is extremely sensitive in this frequency range, a severe noise sensation may result. Hence it is crucial to control vibration and noise in electric motor.

Because noise is generated by vibrating surfaces, noise and vibration in PMSMs can be treated as a single issue. Therefore, vibration control is very important to control noise generation in electric vehicles.

2. LITERATURE REVIEW

- In [1] the spectral characteristics of hybrid electric vehicle (HEV) and internal combustion engine vehicle (ICEV) were compared. A HEV and an ICEV with same engine capacity were selected, with the HEV operating in hybrid mode and ICEV operating in the sixth gear, data collected showed that in the low-frequency region, the A-weighting sound pressure levels (SPLs) of HEV and ICEV are extremely similar. However, HEV's A-weighting SPL is much greater than ICEV in the high-frequency region (in the frequency range of 1100 to 1750 Hz).
- In [2], [3], a comparison of several electric motors was made based on a variety of criteria, and it was discovered that PMSM are among the most ideal devices for EVs and HEVs due to their advantages.
- [4] lists the various vibration sources in PMSM. Special attention is paid to the classification of electromagnetic vibrations and the parameters that influence maxwell forces. In [5] PMSMs are classified depending on the direction of magnetic flux and mechanism of electromagnetic vibration in each of the case is also discussed. Methods for predicting electromagnetic vibration and vibration & noise reduction methods are also presented.
- The modal simulation of the PMSM was performed using the finite element method in [6]. Natural frequencies and associated modes of the motor stator in the free state were computed using reasonable simplification.
- In [7] a multi physics model was developed to compare the vibration and noise in PMSMs with varying slot-pole combinations. The stator vibrations were calculated using mode superposition method and the boundary element method was used for noise calculation.
- The skew factor of stator was chosen as the research variable in [8]. The finite element approach was used to determine the vibration and noise of motors with varying skew factors., and conclusions were derived about how the skew factor of the stator affected motor vibrations. Study on motor vibration reduction according to the stator shape design in a PMSM was done in [9].

- In [10] axial flux PMSM with an external rotor was selected for investigation. Axial force acting on magnet surface was calculated analytical and the analytical results were validated. A study on how current harmonics and dead time effect the vibration and noise was also done.
- The influence of rotor slot shape on PMSM vibration&noise and magnetic field distribution was investigated in [11]. To optimize the magnetic field, three models are presented. By comparing magnetic field and noise results, the best performing rotor slot geometry is chosen.
- For the calculation of radial electromagnetic forces, a hybrid method is proposed in [12]. Results obtained from analytical, numerical and hybrid method are compared to find the effectiveness of each analysis method.
- [13] develops a field reconstruction approach for determining the tangential&radial components of force. The above-mentioned approach is used to produce a stator current waveform that reduces torque ripple and radial force ripple.
- In [14] effect of air gap deformation on radial vibration characteristics of PMSM are investigated. The effects of stator oval and rotor centrifugal deformation on air gap magnetic flux density, electromagnetic force, and torque are investigated and compared.
- Analytical model is derived in [15] to predict radial displacement along the stator teeth. These displacements are then transformed to sound pressure levels. The analytical model's results are validated using numerical solutions and experimental data. In [16], an improved analytical model for calculating the vibration response of the motor is proposed by modelling the stator as a double circular cylindrical shell.
- In [17] numerical procedure is presented to predict noise and vibration in axial flux motor and motor performance test is performed to validate the proposed model. In [18] a magnetoelastic 3D FE model is presented to calculate the magnetic field and vibrations of motor core, including the magnetostrictive effect.

3. OBJECTIVES

The primary goal of this work is to control vibrations in electric vehicles. Specific objectives of this work are.

- To investigate the effect of slot height and slot opening width on PMSM vibration.
- To investigate the effect of slot height and slot opening width on PMSM performance.

4. VIBRATION AND NOISE IN PMSM

4.1 Sources of vibration and noise in PMSM

Based on the nature of their origin vibration and noise in PMSM can be categorized into three main types. (i) mechanical, (ii) aerodynamic and (iii) electromagnetic.

Mechanical Vibrations: Mechanical components of the electric machine, such as fasteners, bolts and bearings, cause this form of vibration. Mechanical vibrations can also be generated by faults made during the design, manufacturing, or assembly stages. One such issue is improper stator and rotor eccentricity. Source detection methods for mechanical vibrations is well established and noise produced by such vibrations is often in the low frequency region, which is less distressing to human perception than the higher frequency range.

Aerodynamic Vibrations: These vibrations are produced by one or more fans and ventilation ducts used in electric vehicle's cooling system. Aerodynamic vibrations generate noise in the low frequency range; however, PMSMs have an air or water cooling system without a fan, thus the contribution of aerodynamic noise is insignificant.

Electromagnetic Vibrations: The electromagnetic forces within the electric motor cause these vibrations. Noise produced by such vibrations lies in the high frequency range. Human perception is sensitive to this frequency range. The majority of vehicle noise is caused by electromagnetic vibrations.

The normal electromagnetic force acting on the surface of stator teeth and permanent magnets causes most electromagnetic noise. Because electromagnetic vibration causes the majority of vehicle noise, this work focuses on electromagnetic vibrations.

4.2 Electromagnetic vibration classification

The electromagnetic forces that induce electromagnetic vibrations within an electric motor are classified into four types (i) maxwell forces (ii) laplace forces (iii) magnetostrictive forces (iv) cogging torque.

Maxwell Forces: These are the electromagnetic forces acting normally to the surface of stator and rotor. Maxwell forces have radial and tangential components. The radial component of maxwell force acts on the surface of stator teeth, causing deformations in the housing. The acting torque is produced by the tangential component of maxwell force, which also causes torque ripple and vibrations in the rotor.

Maxwell forces are affected by a number of factors, some of which are addressed here. Stator shape will have a significant impact on the distribution of electromagnetic forces around the air gap and results in harmonics. Current and voltage harmonics are reflected in the air gap electromagnetic forces and affect the electromagnetic vibrations. Even minor changes in the airgap geometry have a major impact on electromagnetic vibrations because they cause harmonics.

Laplace Forces: These forces act on stator coils, causing them to vibrate and cause insulation difficulties.

Magnetostrictive Forces: Because of the magnetostrictive nature of the electrical steel used to make the stator, when the motor is exposed to a fluctuating strong magnetic field, the stator tends to change shape, causing vibrations in the motor.

Cogging Torque: It is caused by the force of attraction between permanent magnets and stator teeth. It causes motor vibration and jerky sensations.

Of all the above-mentioned forces the vibrations produced by maxwell forces are the major contributor to the motor vibration and noise hence in this work attention is given to maxwell forces.

In radial flux PMSM radial electromagnetic forces produce vibrations. The radial forces acting on the surface of the stator cause housing deformation. Motor housing is the main noise radiator in radial flux PMSM. In axial flux PMSM axial electromagnetic forces produce vibrations. Disk shaped cover is the major noise source in axial flux PMSM.

4.3 Vibration analysis methods

Vibration calculation in PMSM involves electromagnetic field, structure mode, vibration response and is hence a Multiphysics issue. Three main methods are used for vibration analysis in PMSM. (i) numerical method (ii) analytical method (iii) semi analytical method.

In numerical method a finite element software is used to predict vibration and noise. The numerical technique achieves higher precision since it accounts for complex shapes and installation conditions. Because accurate prediction of vibrations requires accurate prediction of electromagnetic forces in three dimensions, the numerical method takes more time and is difficult to forecast vibrations across a wide speed range.

To overcome the limitations of numerical methods many scholars predict vibrations using the analytical methods. Accurate calculation of the surface vibration velocity is key to an analytical model. In the analytical method model shape and frequency calculation is involved and different models are proposed to achieve a higher accuracy and precision. Analytical approaches are appropriate for motors with simple configurations and fail to account for all boundary conditions.

Semi analytical method combines numerical and analytical methods to predict vibrations. The semi analytical method attempts to combine the benefits of numerical and analytical methods while overcoming the limitations of each. Analytical solutions are employed when minimum computing time is required, whereas numerical solutions are used when higher accuracy is required.

4.4 Electromagnetic vibration and noise reduction

Reducing the amplitude of electromagnetic forces will aid in vibration and noise reduction. Avoiding resonance, on the other hand, can help to lessen vibrations and noise.

Fig 2b shows the slot geometry of the stator. In Fig 2b Bs_0 is slot opening width, Bs_1 is slot tip width, Bs_2 is slot base width, Hs_0 is stator tooth tip height and Hs_2 is slot height. Slot opening width, air gap length and thickness of permanent magnets are the geometrical parameters of the PMSM that are sensitive to the amplitude of electromagnetic forces. Because these parameters have little effect on the modal frequencies and performance of the motor, they can be optimized to reduce vibrations and noise while maintaining motor performance.

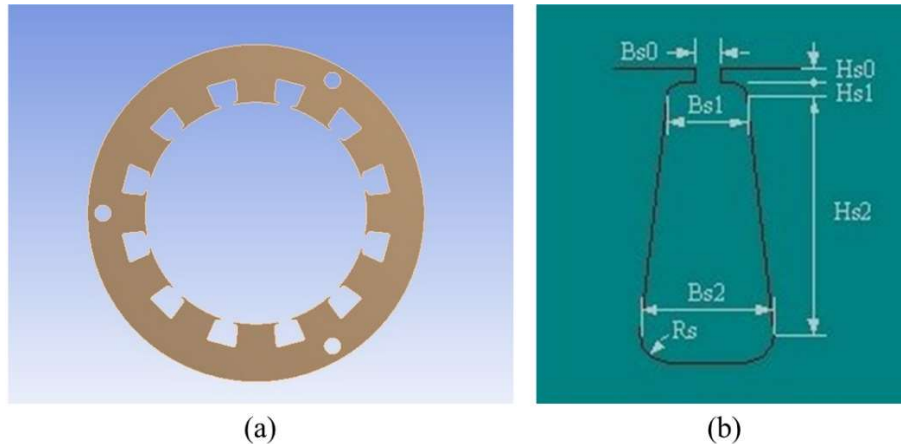


Fig 2: (a)PMSM stator. (b)stator slot geometry.

To reduce motor vibration and torque pulsations, methods such as stator skewing, rotor skewing, notching, and tooth shape modification are used. Motor performance suffers as a result of these procedures. As a result, a compromise between vibration and performance is required. Optimization of the structural characteristics to enhance the gap between modal frequencies and electromagnetic force frequencies can assist reduce vibrations and noise. This strategy is best suited to fixed speed motors.

The optimization of structural parameters sensitive to electromagnetic forces is the most favorable of the three methods listed above, as vibration reduction is achieved with little loss in performance. As a result, the parameters slot height and slot opening width are chosen for investigation in this work.

5. SIMULATION

5.1 Methodology

In this project, a numerical method is used to investigate the effect of stator design parameter on PMSM vibrations. The parameters chosen for analysis are slot height and slot opening width. To investigate the influence of slot height and slot opening width, three stator models with changing values of slot height and three stator models with varying values of slot opening width are built. Vibration analysis is performed on all models.

Ansys electronics suit 19.2 was used to create the structural model, calculate electromagnetic forces, and to calculate and get the distribution of magnetic flux density. Ansys workbench 19.2 was used for modal analysis and harmonic response analysis. Structural model created using Ansys electronics was used as an input for the modal analysis. The modal analysis results and electromagnetic force data are used as inputs to the harmonic response analysis. In harmonic response analysis mode superposition method is used to get the vibration response.

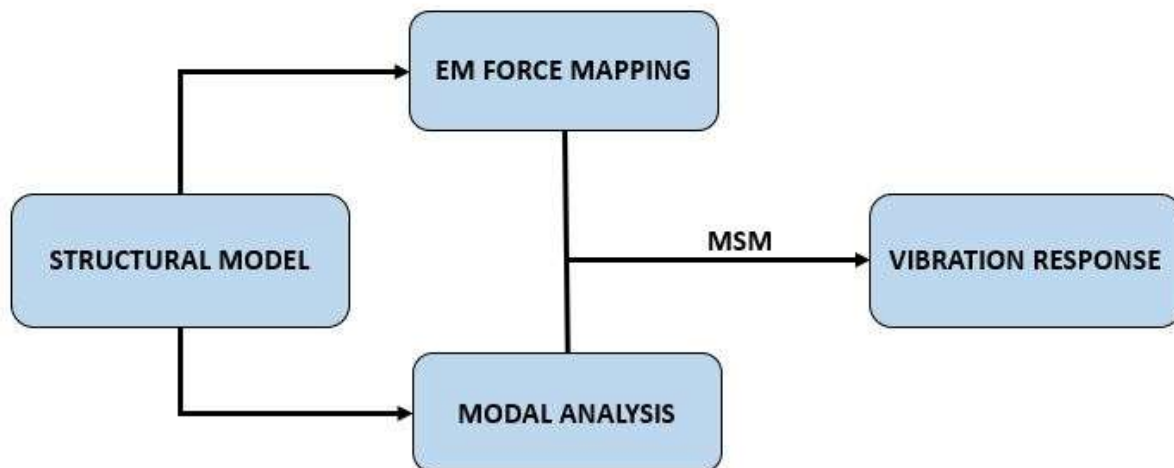


Fig 3: flowchart of vibration analysis.

5.2 Simulation details

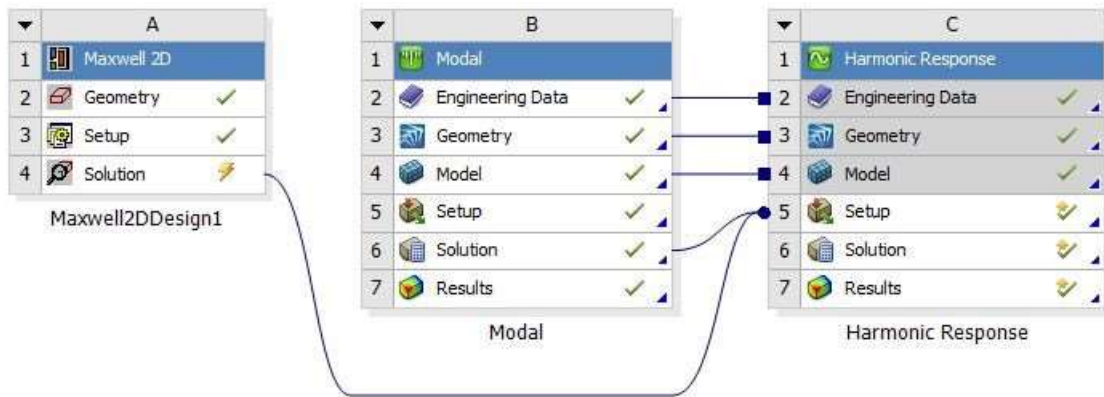


Fig 4: Ansys workbench simulation setup.

Ansys Electronics: The first step in Ansys electronics suit 19.2 is to create the PMSM model. The three-dimensional model of the motor is created using the maxwell 3D design module. Values of many parameters must be specified when creating structural model of the motor. Circuit parameters, stator parameters, rotor parameters, and shaft parameters are the four basic forms of parameter data required. The values of the geometrical parameters of the models constructed to investigate the influence of slot height and slot opening width are presented in the table below.

Table 2: design parameter values for (a) slot height variation. (b) slot opening width variation.

Parameter	model 1	model 2	model 3	Parameter	model 1	model 2	model 3
Stator inner diameter	218	217	216	Stator inner diameter	217	217	217
Stator outer diameter	330	330	330	Stator outer diameter	330	330	330
Slot height	16.5	17	17.5	Slot height	17	17	17
Air gap	4	3.5	3	Slot opening width	10	11	12
Slot opening width	11	11	11	Air gap	3.5	3.5	3.5
Rotor outer diameter	210	210	210	Rotor outer diameter	210	210	210
Rotor inner diameter	145	145	145	Rotor inner diameter	145	145	145
Rotor length	75	75	75	Rotor length	75	75	75
PM width	38	38	38	PM width	38	38	38
PM height	6	6	6	PM height	6	6	6
Number of stator slots	12	12	12	Number of stator slots	12	12	12
Number of poles	14	14	14	Number of poles	14	14	14
Slot top width	23.5	23.5	23.5	Slot top width	23.5	23.5	23.5
Slot base width	29	29	29	Slot base width	29	29	29
Stator tooth tip height	2	2	2	Stator tooth tip height	2	2	2
all values are in (mm)				all values are in (mm)			

(a)

(b)

Following the creation of the geometry, the performance data of the motor model was gathered. To get motor performance statistics, the rated output power was set to 110 kW, the rated voltage to 300 V, and the rated speed to 13300 rpm.

Following performance data, harmonic force data and air gap magnetic flux density data was gathered. Transient setup is required to get the force and magnetic flux density data. Stop time for transient analysis is 0.0012 sec and time step is 6e-06 sec.

Ansys Workbench: The first step in Ansys workbench is modal analysis. Stator model created in Ansys electronics is imported into modal analysis. A cylindrical coordinate system is added at the center of the stator. Meshing is done with adaptive sizing and resolution is set to 6. Three holes, as shown in Fig 5, are at distance of 150mm from the center and have a diameter of 16mm. These holes are made fixed support. Modal analysis is performed using all of the previously described settings.

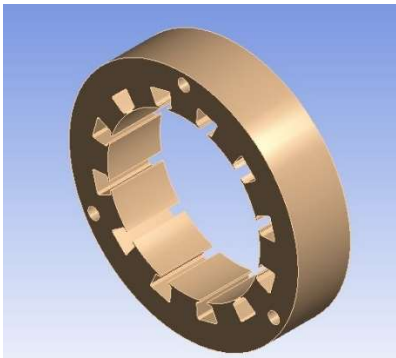


Fig 5: PMSM stator 3D model in isometric view.

Following the modal analysis, the harmonic response analysis was done. Results from modal analysis and electromagnetic force data are used for harmonic response analysis. Remote loads are imported onto the surface of stator teeth. Mode superposition method is used to get the frequency response. In the analysis settings the frequency range is set to 2000 Hz for the minimum frequency and 20000 Hz for the highest frequency and solution interval is set to 50. Finally, frequency response is added and coordinate system is changed to cylindrical coordinate system to get the deformation is radial direction. Harmonic response analysis is performed using all of the previously described settings. Amplitude of vibration vs frequency plot and deformation diagrams are obtained.

6. RESULTS AND DISCUSSIONS

6.1 Modal analysis

Results for slot height variation

Table 3: modal analysis results for slot height variation.

mode	16.5mm	17mm	17.5mm
1	2522.7	2520.2	2517.6
2	2523	2520.4	2517.9
3	2585.5	2582.6	2579.7
4	3005.7	2995.8	2985.3
5	3289.7	3278.6	3267.4
6	3290	3279.1	3268.2
	all values in Hz		

The natural frequency decreases as the slot height values are increased from 16.5mm to 17.5mm for each mode. However, the observed change in natural frequencies is small. The 5th mode exhibits the greatest change in natural frequency, with a difference of 22.3 Hz.

Results for slot opening width variation

Table 4: modal analysis results for slot opening width variation.

mode	10mm	11mm	12mm
1	2519.4	2520.2	2520.9
2	2519.7	2520.4	2521.2
3	2581.5	2582.6	2583.6
4	2992.7	2995.8	2998.7
5	3274.2	3278.6	3282.5
6	3275.3	3279.1	3283.5
	all values in Hz		

The natural frequency is observed to increase as the slot opening width is increased from 10mm to 12mm for each mode. However, the observed change in natural frequencies is small. The 5th mode exhibits the greatest variance in natural frequency, with a difference of 8.3 Hz. When compared with the variation observed in the frequencies of slot height, variations observed in slot opening width are small.

6.2 Amplitude of vibration and motor performance

Results for slot height variation

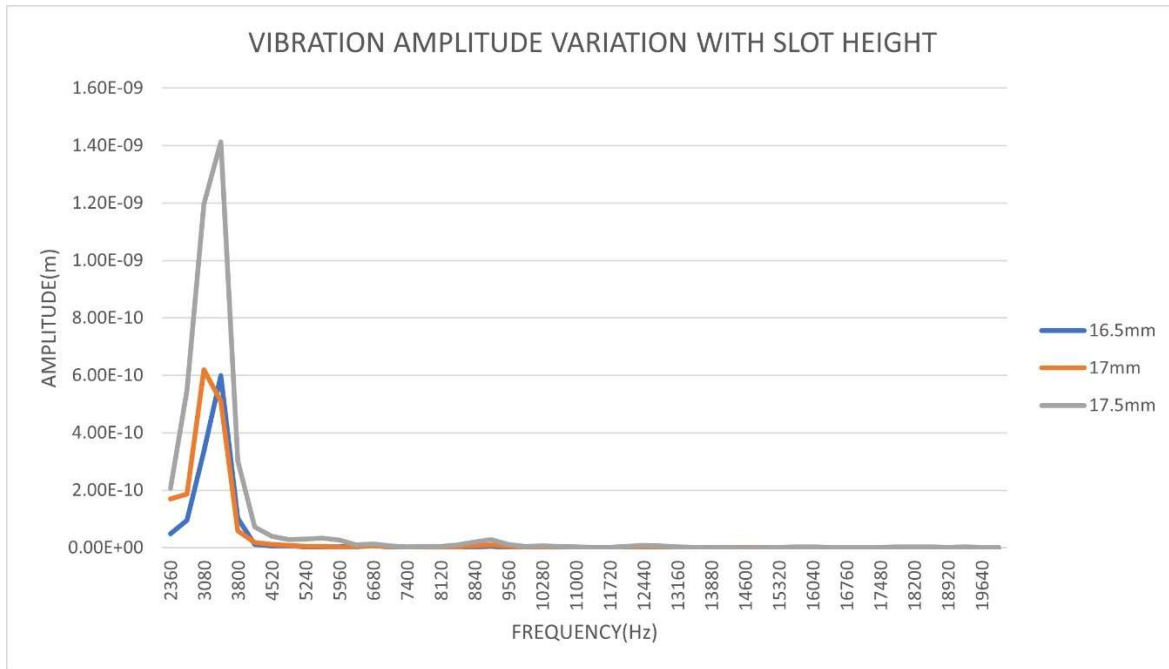


Fig 6: amplitude of vibration variation with slot height.

Amplitude of vibration in radial direction increases as the slot height is increased from 16.5mm to 17.5mm. Amplitudes are measured between 2000 and 20000 Hz. Peak amplitude is 5.99e-10 m in slot height 16.5mm, 6.19e-10 in slot height 17mm, and 1.41e-9 in slot height 17.5mm. From 16.5mm to 17.5mm there is a 135.39% increase in peak amplitude of vibration.

Table 5: motor performance variation with slot height.

	16.5mm	17mm	17.5mm
Output power(W)	92287.7	86612.6	80295.2
Input power(W)	95823.3	90051.8	83528.4
Efficiency(%)	96.3104	96.1808	96.1292
Rated torque(N.m)	66.2619	62.1872	57.6514

Output power, efficiency and rated torque decrease as the slot height is increased from 16.5mm to 17.5mm. From 16.5mm to 17.5mm output power drops by 11992.5 W and rated torque drops by 8.6105 Nm.

Results for slot opening width variation

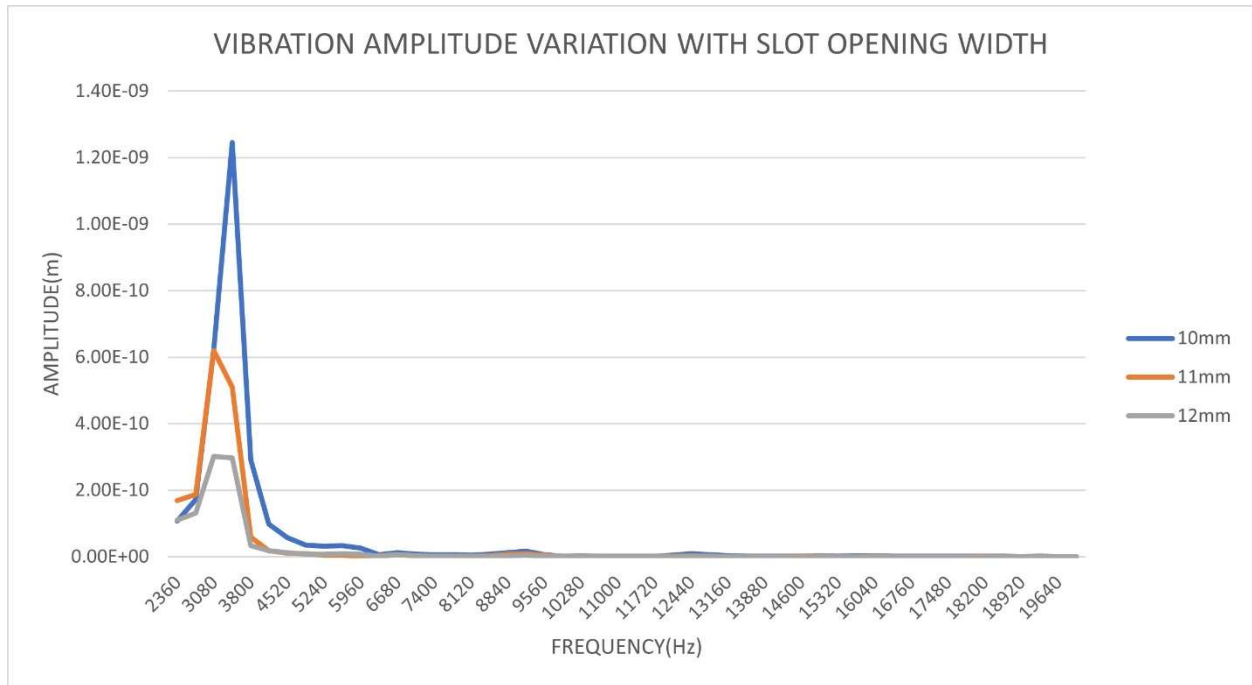


Fig 7: amplitude of vibration variation with slot opening width.

Amplitude of vibration in radial direction decreases as the slot opening width is increased from 10mm to 12mm. Amplitudes are measured between 2000 and 20000 Hz. Peak amplitude is 1.25×10^{-9} m in slot opening width 10mm, 6.19×10^{-10} in slot opening width 11mm, and 3.01×10^{-10} in slot opening width 12mm. From 12mm to 10mm there is a 315.28% increase in peak amplitude of vibration.

Table 6: motor performance variation with slot opening width.

	10mm	11mm	12mm
Output power(W)	86839.1	86612.6	86558
Input power(W)	90286.2	90051.8	90000.2
Efficiency(%)	96.182	96.1808	96.1753
Rated torque(N.m)	62.3498	62.1872	62.2126

Output power, efficiency and rated torque decrease as the slot opening width is increased from 10mm to 12mm. From 10mm to 12mm output power drops by 281.1 W and rated torque drops by 0.1372 Nm. The differences in output power and rated torque detected are so small that they can be ignored.

6.3 Deformation images

Results for slot height variation

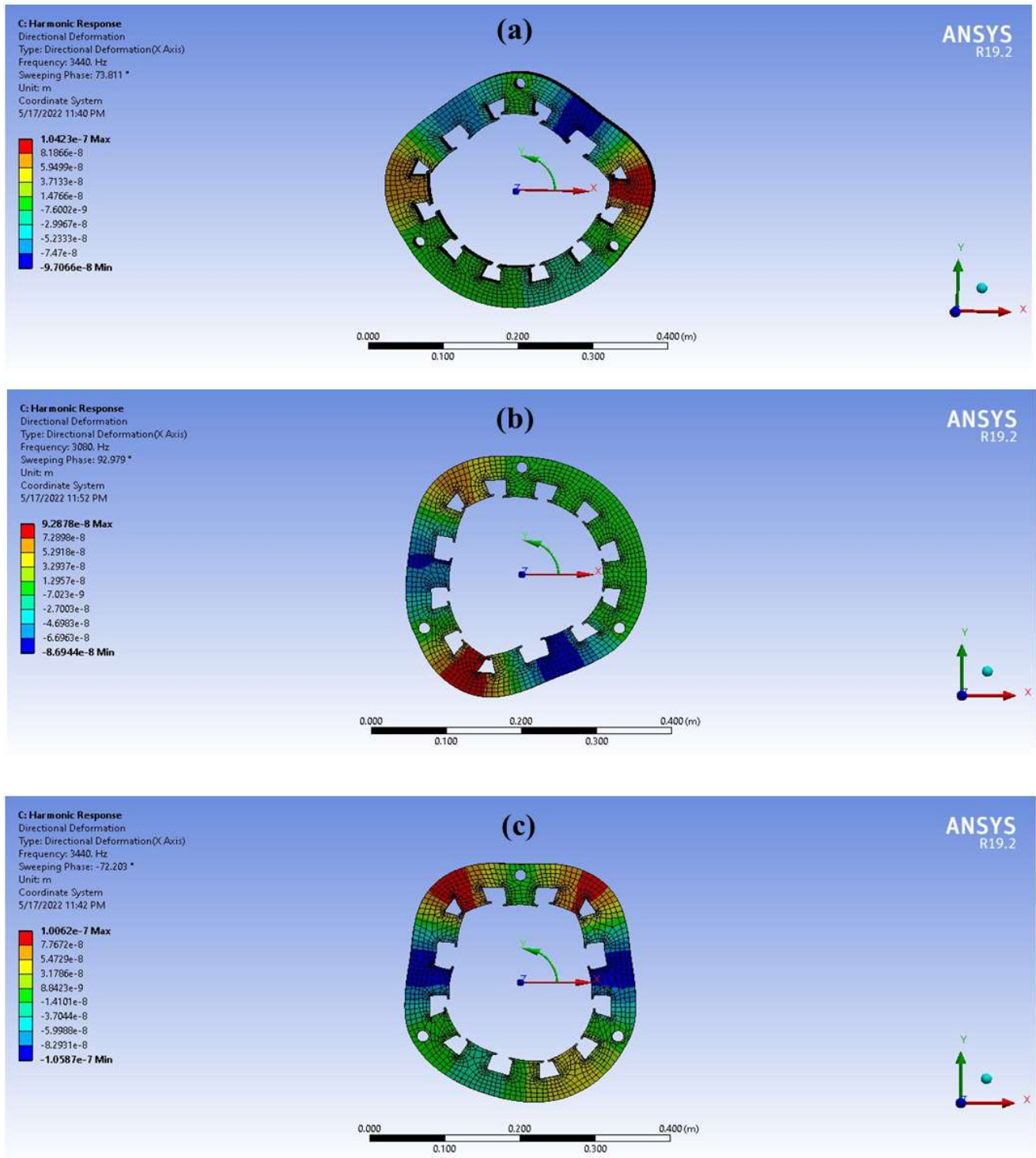


Fig 8: maximum deformation images for slot height (a)16.5mm (b)17mm (c)17.5mm.

Results for slot opening width variation

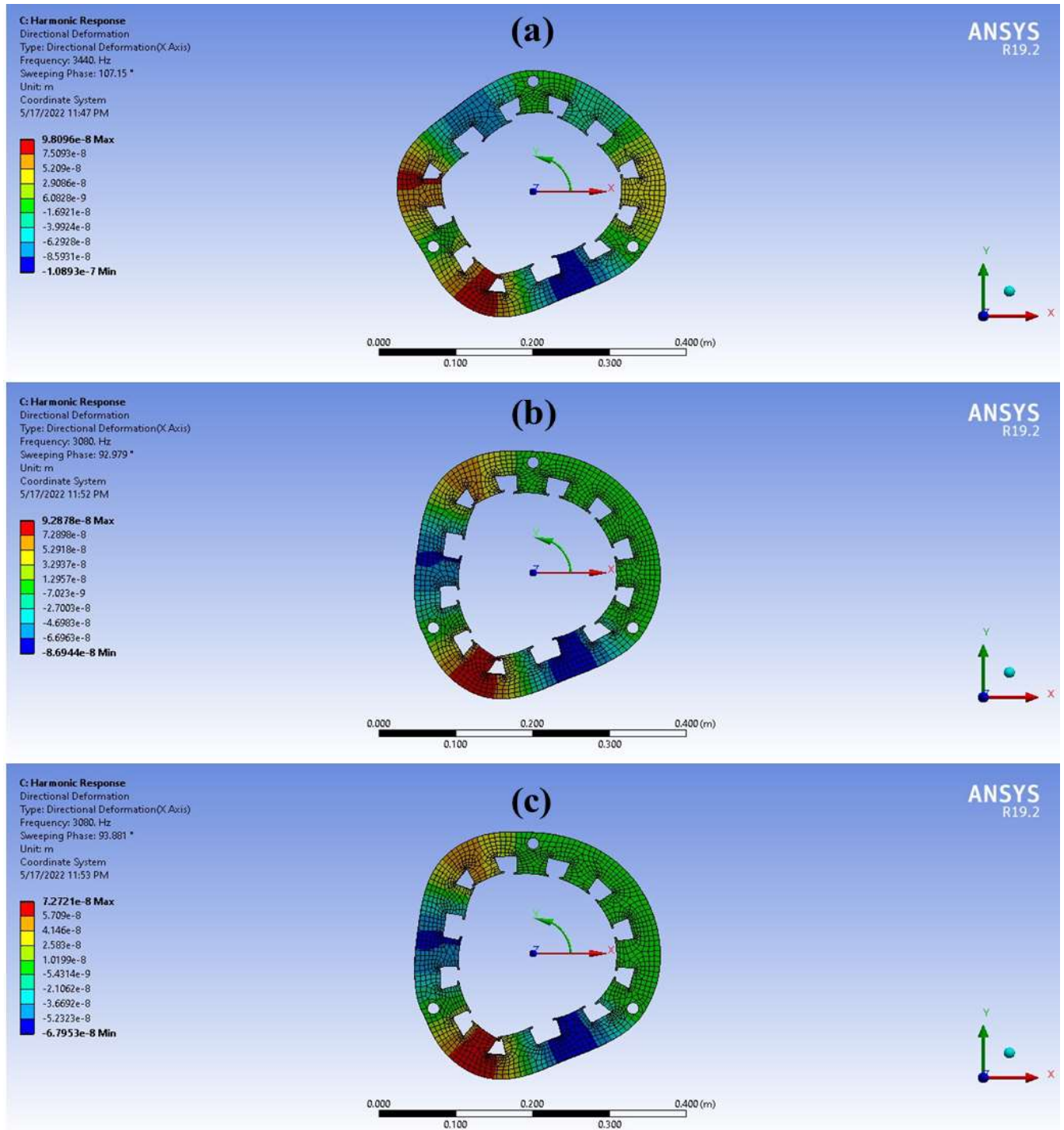


Fig 9: maximum deformation images for slot opening width (a)10mm (b)11mm (c)12mm.

6.4 Radial electromagnetic force

Results for slot height variation



Fig 10: radial force variation with slot height.

Magnitude of radial forces increases as the slot height values are increased. Maximum variation is observed on teeth 4, with a change of 95.3 N.

Results for slot opening width variation



Fig 11: radial force variation with slot opening width.

Magnitude of radial forces increases as the slot height values are increased. Maximum variation is observed on teeth 12, with a change of 8.47 N. Both the plots above represent the maximum value of the radial electromagnetic force.

6.5 Air-gap magnetic flux density

Results for slot height variation

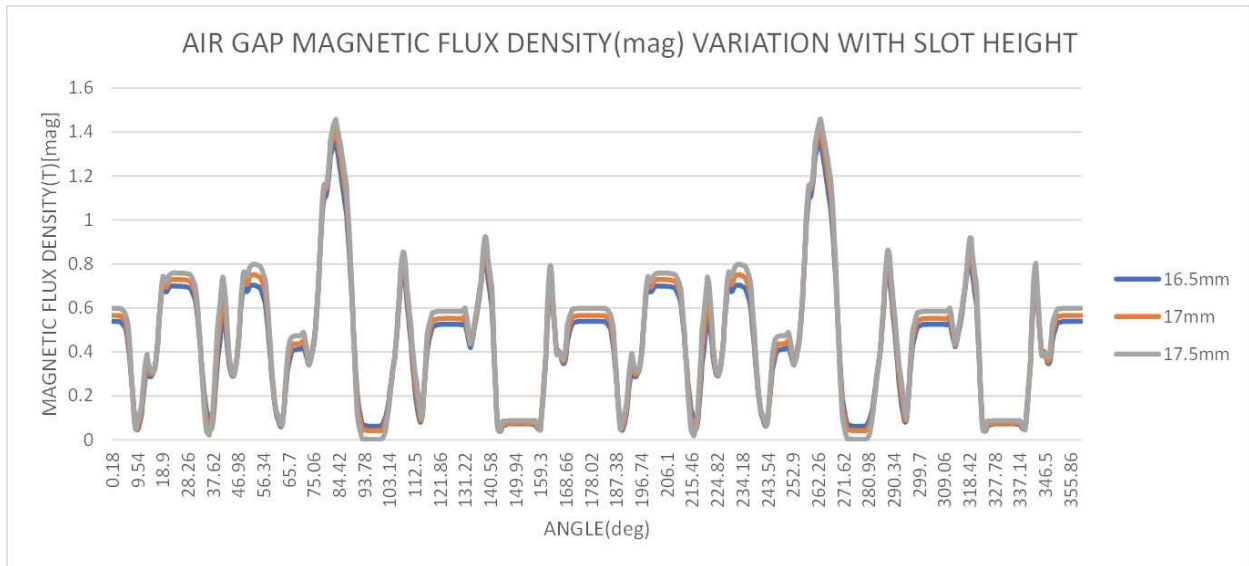


Fig 12: magnitude of airgap magnetic flux density variation with slot height.

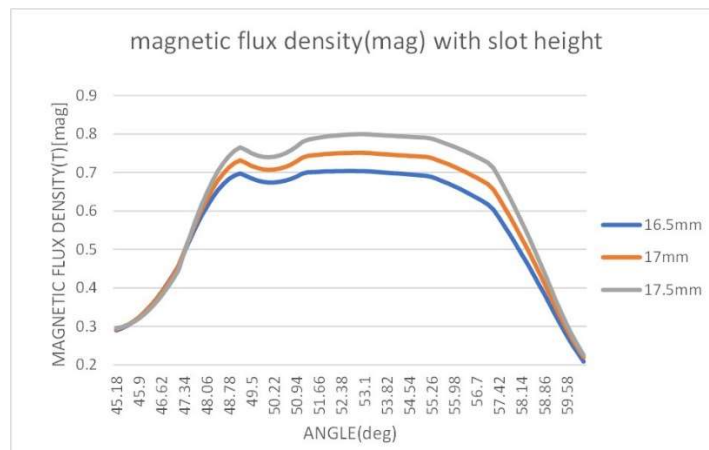


Fig 13: mag_B variation in angle range of 45.18 deg to 60.02 deg.

Magnitude of air gap magnetic flux density increases as the slot height is increased from 16.5mm to 17.5mm. At 53.1 degrees a 13.66 % increase is observed in the magnetic flux density values as the slot height is increased from 16.5mm to 17.5mm.

Results for slot opening width variation

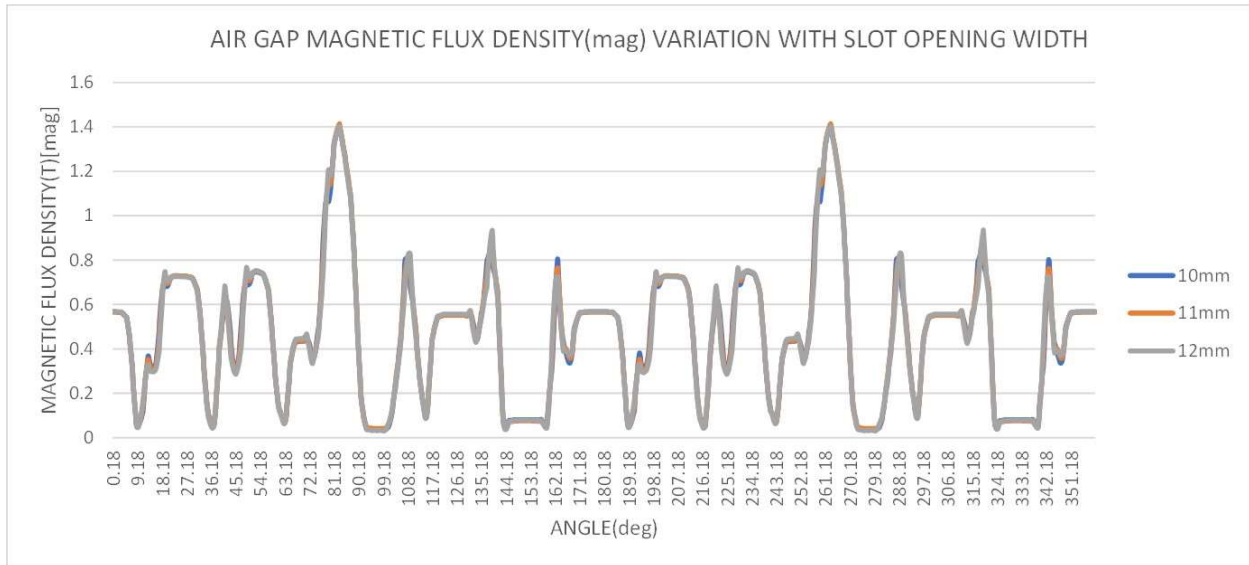


Fig 14: magnitude of airgap magnetic flux density variation with slot height.

Variation observed in the magnitude of air gap flux density as the slot opening width is increased from 10mm to 12mm is so small that it can be neglected. At 53.1 degrees a 0.68% increase in the magnetic flux density values is observed as the slot opening width is increased from 10mm to 12mm.

Magnetic flux density fluctuates with time and along the length of the airgap. Plots in figures 12, 13 and 14 show the variation in magnitude of magnetic flux density along a circle at the center of the airgap. Above plots are drawn at the time of 0.0012 sec.

7. CONCLUSIONS AND SCOPE FOR FUTURE WORK

7.1 Conclusions

The following conclusions can be made from vibration analysis of models with varied values of slot height and slot opening width.

- It is observed that the parameters slot height and slot opening width have an effect on the vibration of PMSM. The amplitude of vibration increases as the slot height increases, and reduces with the increase in slot opening width.
- The parameters slot height and slot opening width also have an effect on output power, efficiency, and rated torque. Output power and rated torque of the motor decrease as the slot height increases. The output power reduces with the increase in slot opening width, but the difference is minor, and the rated torque decreases as well, but the difference is so small that it can be ignored.
- The vibration amplitude increases as slot height increases, and motor performance decreases. However, as slot opening width increases, vibration amplitudes decrease without compromising motor performance much. As a result, having lower slot height values and larger slot opening width values is desirable.
- The percentage change in vibration amplitude observed in slot opening width variation is greater than the change recorded in slot height variation, implying that slot opening width has a greater impact on vibration amplitude than slot height.
- Radial electromagnetic forces acting on the surface of stator teeth and air gap magnetic flux density are affected by the parameters slot height and slot opening width.

7.2 Scope for future work

Effect of only the parameters slot height and slot opening width on motor vibrations is studied in this work. A similar study can be undertaken to determine the effect of other factors on PMSM vibration.

Accurate vibration prediction requires accurate calculation and distribution of electromagnetic forces. There is scope for improvement in the calculation and distribution of electromagnetic forces. Vibrations of a real motor can be recorded, and the results of experimental and analytical vibration data can be compared.

REFERENCES

1. A. K. Putri, S. Rick, D. Franck and K. Hameyer, "Application of Sinusoidal Field Pole in a Permanent-Magnet Synchronous Machine to Improve the NVH Behavior Considering the MTPA and MTPV Operation Area," in *IEEE Transactions on Industry Applications*, vol. 52, no. 3, pp. 2280-2288, May-June 2016, doi: 10.1109/TIA.2016.2532289.
2. A. Lordoglu, M. O. Gulbahce and D. A. Kocabas, "A Comprehensive Disturbing Effect Analysis of Multi-Sectional Rotor Slot Geometry for Induction Machines in Electrical Vehicles," in *IEEE Access*, vol. 9, pp. 49590-49600, 2021, doi: 10.1109/ACCESS.2021.3068821.
3. T. Finken, M. Felden, and K. Hameyer, "Comparison and design of different electrical machine types regarding their applicability in hybrid electrical vehicles," in *Proc. 18th Int. Conf. Electr. Mach.*, Sep. 2008, pp. 1–5.
4. N. Remus et al., "Electromagnetic Noise and Vibration in PMSM and Their Sources: An Overview," 2020 *IEEE Canadian Conference on Electrical and Computer Engineering (CCECE)*, 2020, pp. 1-4, doi: 10.1109/CCECE47787.2020.9255787
5. W. Deng and S. Zuo, "Electromagnetic Vibration and Noise of the Permanent-Magnet Synchronous Motors for Electric Vehicles: An Overview," in *IEEE Transactions on Transportation Electrification*, vol. 5, no. 1, pp. 59-70, March 2019, doi: 10.1109/TTE.2018.2875481.
6. H. Li, D. Zhang, P. Xu, C. Cao, D. Hu, X. Yan, Z. Song, and Z. Hu, "Analysis on the vibration modes of the electric vehicle motor stator," *Vibroengineering PROCEDIA*, vol. 22, pp. 81–86, 2019.
7. F. Lin, S. Zuo, and X. Wu, "Electromagnetic vibration and noise analysis of permanent magnet synchronous motor with different slot pole combinations," *IET Electr. Power Appl.*, vol. 10, no. 9, pp. 900–908, Nov 2016.
8. Z. Han, J. Liu, C. Gong, and J. Lu, "Influence mechanism on vibration and noise of PMSM for different structures of skewed stator," in *proceedings of 20th International Conference on Electrical Machines and Systems*, 2017.
9. H. Kim, T. Lee, S. Kwon and J. Hong, "Vibration analysis according to stator shape design in a PMSM," 2010 *International Conference on Electrical Machines and Systems*, 2010, pp. 1235-1238.

10. W. Deng and S. Zuo, "Axial Force and Vibroacoustic Analysis of External-Rotor Axial-Flux Motors," in *IEEE Transactions on Industrial Electronics*, vol. 65, no. 3, pp. 2018-2030, March 2018, doi: 10.1109/TIE.2017.2739697.
11. Jun Shen, Xuejun Chen, Zhixin Cui, and Lin Ma, "Optimization Design and Research on Vibration and Noise of Permanent Magnet Synchronous Motor for Vehicle," *Progress In Electromagnetics Research M*, Vol. 100, 105-115, 2021, doi:10.2528/PIERM20102711.
12. T. Dai, H. Li, J. Li, B. Yuan and X. Liu, "A Hybrid Calculation Method of Radial Electromagnetic Force Based on Finite Element Method and Analytic Method in A Permanent Magnet Synchronous Machine," 2019 22nd International Conference on Electrical Machines and Systems (ICEMS), 2019, pp. 1-4, doi: 10.1109/ICEMS.2019.8921891.
13. Weidong Zhu, B. Fahimi and S. Pekarek, "A field reconstruction method for optimal excitation of permanent magnet synchronous machines," in *IEEE Transactions on Energy Conversion*, vol. 21, no. 2, pp. 305-313, June 2006, doi: 10.1109/TEC.2005.859979.
14. F. Chai, Y. Li, Y. Pei and Y. Yu, "Analysis of Radial Vibration Caused by Magnetic Force and Torque Pulsation in Interior Permanent Magnet Synchronous Motors Considering Air-Gap Deformations," in *IEEE Transactions on Industrial Electronics*, vol. 66, no. 9, pp. 6703-6714, Sept. 2019, doi: 10.1109/TIE.2018.2880707.
15. R. Islam and I. Husain, "Analytical Model for Predicting Noise and Vibration in Permanent-Magnet Synchronous Motors," in *IEEE Transactions on Industry Applications*, vol. 46, no. 6, pp. 2346-2354, Nov.-Dec. 2010, doi: 10.1109/TIA.2010.2070473.
16. Alex McCloskey, Xabier Arrasate, Xabier Hernández, Iratxo Gómez, Gaizka Almandoz, Analytical calculation of vibrations of electromagnetic origin in electrical machines, *Mechanical Systems and Signal Processing*, Volume 98, 2018, Pages 557-569, ISSN 0888-3270.
17. S. Park, W. Kim and S. Kim, "A Numerical Prediction Model for Vibration and Noise of Axial Flux Motors," in *IEEE Transactions on Industrial Electronics*, vol. 61, no. 10, pp. 5757-5762, Oct. 2014, doi: 10.1109/TIE.2014.2300034.

18. L. Zhu, B. Wang, R. Yan, Q. Yang, Y. Yang and X. Zhang, "Electromagnetic Vibration of Motor Core Including Magnetostriction Under Different Rotation Speeds," in IEEE Transactions on Magnetics, vol. 52, no. 3, pp. 1-4, March 2016, Art no. 8102004, doi: 10.1109/TMAG.2015.2497738.